

Synthetic, Dynamic Nuclear Magnetic Resonance and Crystallographic Studies of Platinum Complexes containing Silyl-substituted Dialkenyl-thioether and -selenoether Ligands†

Edward W. Abel,^a Julian R. Koe,*^{†,‡} Michael B. Hursthouse,^b K. M. Abdul Malik^b and Mohammed A. Mazid^b

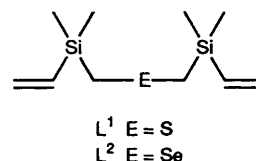
^a Department of Chemistry, The University, Exeter EX4 4QD, UK

^b School of Chemistry and Applied Chemistry, University of Wales College of Cardiff, PO Box 912, Cardiff CF1 3TB, UK

Potentially quadridentate di(silaalkenyl) chalcogenoether ligands have been observed to bind in a bidentate mode *via* an alkene moiety and a chalcogen lone pair of electrons to platinum(II) and in a tridentate mode to rhodium(I) metal centres, *via* the chalcogen atom and both alkene moieties. Variable-temperature NMR studies established the occurrence of fluxional processes in these complexes, the energy barriers of which have been evaluated for the platinum systems. The crystal structures of two species have been determined: $[\text{PtI}_2\{\text{S}(\text{CH}_2\text{SiMe}_2\text{CH}=\text{CH}_2)_2\}]$ forms monoclinic crystals of space group $P2_1/a$ with $a = 12.279(5)$, $b = 8.961(3)$, $c = 18.575(3)$ Å, $\beta = 108.49(2)^\circ$ and $Z = 4$ and $[\{\text{RhCl}\{\text{S}(\text{CH}_2\text{SiMe}_2\text{CH}=\text{CH}_2)_2\}_2]$ forms triclinic crystals of space group $P\bar{1}$ with $a = 7.7178(12)$, $b = 10.289(4)$, $c = 10.5932(14)$ Å, $\alpha = 92.56(2)$, $\beta = 99.544(14)$, $\gamma = 105.26(2)^\circ$ and $Z = 1$. The platinum complex is monomeric and has a square-planar geometry with the iodine atoms in *cis* positions, whilst the rhodium complex is a centrosymmetric dimer with two chlorine atoms bridging a pair of rhodium atoms, both having trigonal-bipyramidal geometry.

Transition-metal complexes of alkenyl thioethers were first investigated in the 1960s,^{1–3} though without the benefit of modern instrumentation to assist in fully deducing the fluxionality and stereochemistry of the systems. The ligands were considered able to bind through both functionalities to metals. Further work^{4–7} in the following two decades established the geometry of the chelate chain more rigorously using X-ray crystallography and variable-temperature ^1H NMR spectroscopy, and two fluxional processes were noted: pyramidal atomic inversion of the co-ordinated sulfur atom and labilisation of the co-ordinated alkene moiety. The effects of introducing a quaternary carbon or silicon atom into the chelate chain of certain butenyl thioether complexes were also investigated⁴ in an attempt to enhance the chelation tendency (*gem* dialkyl effect⁸) and to facilitate analysis by NMR spectroscopy. On the basis of infrared results it was considered that the metal–alkene interaction was weaker for the vinylsilane than for its carbon analogue, and the NMR data were interpreted in the light of this, postulating a stronger metal-to-alkene π back-bond into a hybridised alkene π^* –silicon 3d orbital, but much weaker alkene-to-metal σ bond.

In a series of papers,^{9–13} we have investigated the chemistry, structure and fluxionality exhibited by platinum metal complexes containing both monoalkenyl- and dialkenyl-thioether and -selenoether ligands. The dialkenyl chalcogenoether ligands are potentially quadridentate by virtue of the two donor alkene functions and the two lone pairs of electrons on the chalcogen atom. In complexes with rhodium(I), all four donor sites may be used in forming cyclic trimers¹² containing chalcogen-bridged trigonal-bipyramidal rhodium centres, the metal attaining its most stable configuration with an 18 electron shell. In contrast,



for the bis[dimethylplatinum(II)] species,¹³ which contains two metal centres bridged by a single (quadridentate) ligand, the two functionalities bind to each metal atom (one chalcogen lone pair and one alkene moiety), thus linking the platinum atoms more strongly. In all the platinum and palladium dihalide complexes^{9,10} the ligands were bound in a bidentate manner *via* a chalcogen lone pair and an alkene moiety, except for the dipropenyl thioether ligand for which chelation would have required unacceptable metallacycle ring strain. The bidentate complexes are fluxional, exhibiting both chalcogen inversion and exchange between pendant and co-ordinated alkene moieties.

The current work attempts to clarify the difference between silyl-substituted alkene chain ligands and non-substituted ligands by comparing the thermodynamic parameters in the fluxional process of alkene exchange in the two cases.

Results and Discussion

Preparation and Properties of the Complexes.—The di(silaalkenyl) chalcogenoether ligands L^1 and L^2 were prepared by addition of (chloromethyl)dimethyl(vinyl)silane to an aqueous solution of the chalcogenide anion and reacted readily in equimolar proportions with potassium tetrachloroplatinate(II) in aqueous ethanolic solution left stirring overnight to form the dichloroplatinum complexes. The corresponding bromo- and iodo-derivatives were prepared by metathesis in warm acetone solution. The complexes are all crystalline, soluble in organic solvents and stable to air and moisture. The chloro complexes

† Present address: Materials and Devices Research Laboratory I, Toshiba Corporation, Research and Development Centre, 1 Komukai Toshiba-cho, Saiwai-ku, Kawasaki 210, Japan.

‡ Supplementary data available: see Instructions for Authors, *J. Chem. Soc., Dalton Trans.*, 1994, Issue 1, pp. xxiii–xxviii.

are pale yellow and the colour darkens progressively for the bromo- and iodo-species.

The rhodium(i) complexes were synthesised by addition of two equivalents of the ligand to a cold (-80°C) stirred suspension of the bis(ethylene)rhodium(i) chloride dimer in dichloromethane and stirring for 24 h, allowing the solution gradually to warm to room temperature. The complexes are red-brown, crystalline and moderately soluble in common organic solvents, although they decompose slowly in moisture and air. Addition of two equivalents of triphenylphosphine to a cold (-20°C) solution of the dimeric chloro-rhodium complex $[(\text{RhClL}^1)_2]$ in dichloromethane yields a dark yellow, crystalline 1:1 adduct.

Infrared and analytical data for the complexes are reported in Table 1. The complexes have been further examined by ^1H , ^{13}C and ^{29}Si NMR spectroscopy and ^1H variable-temperature NMR to probe their fluxional properties. To aid in the understanding of the fluxional properties and to investigate the bonding mode of the vinylsilane moiety, crystal-structure analyses were undertaken for representative platinum and rhodium species: $[\text{PtI}_2\{\text{S}(\text{CH}_2\text{SiMe}_2\text{CH}=\text{CH}_2)_2\}]$ and $[(\text{RhCl}\{\text{S}(\text{CH}_2\text{SiMe}_2\text{CH}=\text{CH}_2)_2\})_2]$ respectively.

Crystal Structure of cis-Diiodo(3,3,7,7-tetramethyl-5-thia-3,7-disilano-1,8-diene)platinum(II), $[\text{PtI}_2\text{L}^1]$.—The molecular structure of $[\text{PtI}_2\text{L}^1]$ determined by single-crystal X-ray

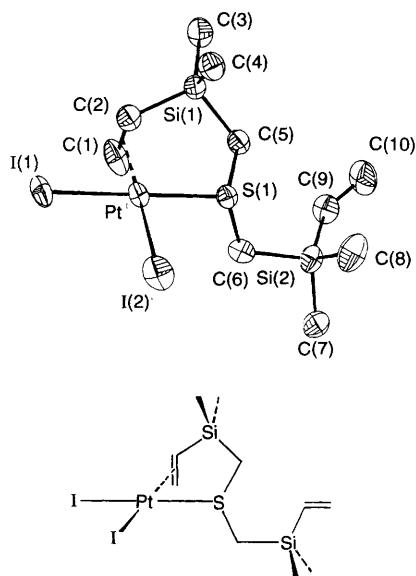


Fig. 1 Crystal structure of *cis*-diiodo(3,3,7,7-tetramethyl-5-thia-3,7-disilano-1,8-diene)platinum(II), $[\text{PtI}_2\text{L}^1]$

diffraction is shown in Fig. 1; selected intramolecular bond lengths and angles are given in Table 2. The fractional atomic coordinates are given in Table 3. The complex is essentially square planar in the solid state with respect to the *cis* iodine atoms, the sulfur atom and the centroid of the co-ordinated alkene, which is oriented almost perpendicularly to the plane. In these respects the structure is similar to that of $[\text{PtI}_2\{\text{S}(\text{CH}_2\text{CH}_2\text{CH}=\text{CH}_2)_2\}]$,¹⁰ the ligand binding in a bidentate mode in each case with the pendant alkenyl chain pseudoaxially oriented at sulfur with respect to the metallacycle plane. This configuration at the chalcogen atom allows the adjacent carbon atom [C(6)] in the pendant chain to be positioned further from the large iodine atoms and also removes the bulky dimethyl-(vinyl)silyl group from the co-ordination sphere of the metal to the least sterically congested location.

The co-ordinated alkene centroid to platinum bond in $[\text{PtI}_2\text{L}^1]$ has a length of 2.052(14) Å and is somewhat shorter than that observed in $[\text{PtI}_2\{\text{S}(\text{CH}_2\text{CH}_2\text{CH}=\text{CH}_2)_2\}]$ (2.086 Å). The platinum-sulfur bond length of 2.287(3) Å is typical of that observed^{9,10} in other similar compounds, e.g. in $[\text{PtI}_2\{\text{S}(\text{CH}_2\text{CH}_2\text{CH}=\text{CH}_2)_2\}]$ it is 2.280 Å and in $[\text{PtBr}_2\{\text{MeS}(\text{CH}_2)_3\text{CH}=\text{CH}_2\}]$ it is 2.286 Å. The dimethylsilyl moiety is positioned and oriented analogously to the methylene group in $[\text{PtI}_2\{\text{S}(\text{CH}_2\text{CH}_2\text{CH}=\text{CH}_2)_2\}]$ and the increased bond distances to both adjacent carbon atoms (1.86 Å, cf. 1.5 Å in the dibutenyl thioether complex) result only in a slight twisting of the alkene moiety about the metal-centroid axis, forcing the more substituted end of the alkene further away from the chalcogen atom in order to accommodate the increase in bonding distances. The increase in double bond length upon co-ordination of the alkene, Δd , is 0.13 Å for $[\text{PtI}_2\text{L}^1]$, rather less than in $[\text{PtI}_2\{\text{S}(\text{CH}_2\text{CH}_2\text{CH}=\text{CH}_2)_2\}]$ (0.19 Å). Since co-ordination of an alkene to a metal effectively reduces the C=C bond strength, a greater Δd should reflect a greater degree of metal-alkene π interaction. It thus appears that for the vinylsilane, compared to its unsubstituted analogue, the metal-alkene bond is slightly weaker. (This point is discussed further in the NMR section.)

Crystal Structure of Di- μ -chlorobis[3,3,7,7-tetramethyl-5-thia-3,7-disilano-1,8-diene]rhodium(I), $[(\text{RhClL}^1)_2]$.—The complex is observed to adopt a dimeric, chloride-bridged structure with pseudo-trigonal-bipyramidal geometry at the rhodium centres, a crystallographic centre of inversion and a non-crystallographic mirror plane containing the Rh_2Cl_2 unit, as is evident in Fig. 2. Selected bond lengths and angles are in Table 4 and the fractional atomic coordinates are in Table 5. The axial sites are occupied by a chlorine atom and a sulfur atom, the aliphatic chains of which chelate to the same rhodium atom *via* both alkenyl groups, which occupy equatorial sites, oriented in the trigonal plane with the terminal atoms nearest

Table 1 Characterisation of compounds

Sample	Nature	M.p./ $^{\circ}\text{C}$	Analysis ^a (%)		Alkene stretch ^b /cm ⁻¹	
			C	H	Co-ordinated	Unco-ordinated
L^1	Malodorous oil		52.15 (52.10)	8.60 (8.60)	—	1596
L^2	Malodorous oil		43.60 (43.30)	7.75 (8.00)	—	1594
$[\text{PtCl}_2\text{L}^1]$	Pale yellow crystals	130	24.00 (24.20)	4.45 (4.45)	1485	1595
$[\text{PtBr}_2\text{L}^1]$	Yellow crystals	122	20.35 (20.50)	3.70 (3.80)	1482	1594
$[\text{PtI}_2\text{L}^1]$	Dark yellow crystals	89	17.65 (17.70)	3.20 (3.25)	1477	1591
$[\text{PtCl}_2\text{L}^2]$	Pale yellow crystals	110 ^c	21.95 (22.10)	4.00 (4.10)	1491	1595
$[\text{PtBr}_2\text{L}^2]$	Yellow crystals	109 ^c	18.70 (19.00)	3.45 (3.50)	1482	1594
$[\text{PtI}_2\text{L}^2]$	Dark yellow crystals	112 ^d	16.45 (16.55)	2.85 (3.05)	1482	1594
$[(\text{RhClL}^1)_2]$	Red crystals	155 ^d	32.65 (32.55)	5.95 (6.00)	1474	—
$[(\text{RhClL}^2)_2]$	Red crystals	150 ^d	28.70 (28.90)	5.40 (5.35)	1471	—
$[\text{RhClL}^1(\text{PPh}_3)]$	Dark yellow crystals	129	52.90 (53.30)	5.70 (5.90)	1483	1587

^a Calculated values in parentheses. ^b Ligand samples as liquid films; complexes as KBr discs. ^c Melts and decomposes. ^d Decomposes.

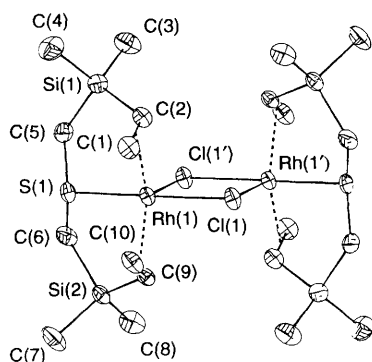
Table 2 Selected bond lengths (Å) and angles (°) for [PtI₂L¹]

Pt–I(1)	2.5921(14)	Pt–I(2)	2.5770(13)
Pt–S(1)	2.287(3)	Pt–C(1)	2.143(15)
Pt–C(2)	2.191(14)	S(1)–C(5)	1.786(13)
S(1)–C(6)	1.788(12)	Si(1)–C(2)	1.86(2)
Si(1)–C(4)	1.86(2)	Si(1)–C(5)	1.867(12)
Si(1)–C(3)	1.87(2)	Si(2)–C(8)	1.81(2)
Si(2)–C(7)	1.82(2)	Si(2)–C(9)	1.87(2)
Si(2)–C(6)	1.875(14)	C(1)–C(2)	1.39(2)
C(9)–C(10)	1.26(2)	Pt–C(01)*	2.052(14)
S(1)–Pt–I(2)	85.58(9)	S(1)–Pt–I(1)	173.25(9)
I(2)–Pt–I(1)	90.68(5)	I(2)–Pt–C(01)	90.6(5)
I(2)–Pt–C(01)	174.1(5)	S(1)–Pt–C(01)	93.7(5)
C(5)–S(1)–C(6)	103.6(6)	C(5)–S(1)–Pt	105.9(4)
C(6)–S(1)–Pt	109.7(5)	C(2)–Si(1)–C(4)	108.9(7)
C(2)–Si(1)–C(5)	102.3(6)	C(4)–Si(1)–C(5)	112.4(7)
C(2)–Si(1)–C(3)	112.7(7)	C(4)–Si(1)–C(3)	112.5(8)
C(5)–Si(1)–C(3)	107.6(7)	C(8)–Si(2)–C(7)	112.1(8)
C(8)–Si(2)–C(9)	110.9(9)	C(7)–Si(2)–C(9)	109.6(8)
C(8)–Si(2)–C(6)	109.8(7)	C(7)–Si(2)–C(6)	105.2(7)
C(9)–Si(2)–C(6)	109.0(7)	C(1)–C(2)–Si(1)	121.6(12)
S(1)–C(5)–Si(1)	107.2(7)	S(1)–C(6)–Si(2)	115.7(7)
C(10)–C(9)–Si(2)	126(2)		

* C(01) is the centroid of the co-ordinated C(1)=C(2) double bond.

Table 3 Atomic coordinates ($\times 10^4$) for [PtI₂L¹]

Atom	x	y	z
Pt	9 058.9(4)	2 709.0(6)	2 180.1(3)
I(1)	8 323.6(12)	134.7(12)	1 587.2(7)
I(2)	8 627.6(12)	1 991.5(16)	3 405.7(7)
S(1)	9 500(3)	5 015(4)	2 722(2)
Si(1)	8 796(4)	5 597(5)	1 080(2)
Si(2)	11 347(3)	6 738(5)	3 980(2)
C(1)	10 110(16)	2 922(17)	1 458(9)
C(2)	9 047(14)	3 552(18)	1 070(8)
C(3)	9 230(16)	6 615(18)	334(8)
C(4)	7 266(12)	5 931(19)	1 005(9)
C(5)	9 807(12)	6 160(15)	2 023(6)
C(6)	10 840(11)	4 935(15)	3 472(7)
C(7)	12 539(14)	6 230(22)	4 818(8)
C(8)	10 181(17)	7 616(22)	4 227(10)
C(9)	11 878(13)	7 983(20)	3 354(9)
C(10)	11 572(18)	9 309(22)	3 177(11)

**Fig. 2** Crystal structure of di- μ -chlorobis[(3,3,7,7-tetramethyl-5-thia-3,7-disilanon-1,8-diene)rhodium(II)], [RhClL¹]₂

each other. The co-ordination sphere of rhodium is completed by planar chloride-bridge formation upon dimerisation, an electron pair being accepted into the third equatorial site from the axial chlorine of the dimerising complex.

The local geometry at the rhodium atom thus closely resembles that in mononuclear five-co-ordinate rhodium complexes such as [RhCl(Ph₂PCH₂CH₂CH=CH₂)₂]¹⁴ and [RhCl{P(CH₂CH₂CH=CH₂)₃}]¹⁵ which have respectively

Table 4 Selected bond lengths (Å) and angles (°) for [(RhClL¹)₂]^a

Rh(1)–S(1)	2.2595(9)	Rh(1)–Cl(1)	2.3918(9)
Rh(1)–Cl(1')	2.588(1)	Rh(1)–C(1)	2.141(4)
Rh(1)–C(2)	2.184(4)	Rh(1)–C(01) ^b	2.047(4)
Rh(1)–C(9)	2.192(4)	Rh(1)–C(10)	2.126(4)
Rh(1)–C(02) ^b	2.043(4)	S(1)–C(6)	1.800(4)
S(1)–C(5)	1.804(5)	Si(1)–C(2)	1.847(4)
Si(1)–C(3)	1.846(5)	Si(1)–C(4)	1.855(5)
Si(1)–C(5)	1.893(4)	Si(2)–C(8)	1.843(5)
Si(2)–C(9)	1.844(4)	Si(2)–C(7)	1.858(5)
Si(2)–C(6)	1.894(5)	C(1)–C(2)	1.398(6)
C(9)–C(10)	1.401(6)		
S(1)–Rh(1)–Cl(1)	179.71(3)	Cl(1)–Rh(1)–Cl(1')	86.08(3)
S(1)–Rh(1)–Cl(1')	93.76(3)	C(01)–Rh(1)–Cl(1)	90.34(9)
C(01)–Rh(1)–Cl(1')	112.67(9)	C(01)–Rh(1)–S(1)	89.50(9)
C(02)–Rh(1)–Cl(1)	90.67(9)	C(02)–Rh(1)–Cl(1')	114.03(9)
C(02)–Rh(1)–S(1)	89.62(9)	C(02)–Rh(1)–C(01) ^b	133.25(9)
Rh(1)–Cl(1')–Rh(1)	93.92(3)	C(6)–S(1)–C(5)	104.3(2)
C(6)–S(1)–Rh(1)	103.72(14)	C(5)–S(1)–Rh(1)	103.74(13)
C(2)–Si(1)–C(3)	112.2(2)	C(2)–Si(1)–C(4)	111.8(2)
C(3)–Si(1)–C(4)	109.7(3)	C(2)–Si(1)–C(5)	107.1(2)
C(3)–Si(1)–C(5)	106.4(2)	C(4)–Si(1)–C(5)	109.5(2)
C(8)–Si(2)–C(9)	110.6(2)	C(8)–Si(2)–C(7)	110.6(3)
C(9)–Si(2)–C(7)	110.9(2)	C(8)–Si(2)–C(6)	109.4(2)
C(9)–Si(2)–C(6)	107.3(2)	C(7)–Si(2)–C(6)	108.0(2)
C(1)–C(2)–Si(1)	123.4(3)	S(1)–C(5)–Si(1)	110.1(2)
S(1)–C(6)–Si(2)	108.7(2)	C(10)–C(9)–Si(2)	123.4(3)

^a Symmetry transformations used to generate equivalent atoms (dashed) belonging to same dimeric molecule: 1 – x, 1 – y, 2 – z.^b C(01) is the centroid of co-ordinated double bond C(1)=C(2); C(02) is the centroid of C(9)=C(10).**Table 5** Atomic coordinates ($\times 10^4$) for [(RhClL¹)₂]

Atom	x	y	z
Rh(1)	4276.8(3)	4567.3(3)	8272.3(2)
Cl(1)	6914(1)	4546(1)	9809(1)
S(1)	1777(1)	4581(1)	6827(1)
Si(1)	509(2)	2053(1)	8166(1)
Si(2)	3971(2)	7494(1)	7164(1)
C(1)	4069(6)	2557(4)	7514(4)
C(2)	3026(6)	2442(4)	8485(4)
C(3)	–449(7)	1811(6)	9651(5)
C(4)	–559(8)	545(5)	6995(6)
C(5)	–94(5)	3583(4)	7489(4)
C(6)	1614(6)	6287(4)	7046(4)
C(7)	4221(8)	8008(6)	5530(5)
C(8)	4214(7)	8981(5)	8283(5)
C(9)	5646(5)	6572(4)	7764(3)
C(10)	6000(6)	5543(4)	7023(4)

two and three alkene moieties co-ordinated to the metal atom and oriented in the equatorial plane of the trigonal-bipyramidal co-ordination sphere. Molecular orbital calculations¹⁶ have clearly shown that co-ordination of the alkene in the equatorial plane leads to maximum metal–alkene π^* back-bonding. Trigonal-pyramidal local geometry was also observed¹² in the similarly prepared complex [(RhCl{Se(CH₂CH₂CH=CH₂)₂}]₃ though this species, containing an unsubstituted dialkenyl selenoether ligand, forms a cyclic trimer with alternating rhodium and selenium atoms, in marked contrast to the present complex which dimerises, probably as a result of the increased steric hindrance of the bulky dimethylsilyl group. The ligand is thus tridentate and affords the first example of this bonding mode for dialkenyl chalcogenoether ligands, previously observed to bind in only bi- or tetra-dentate modes.^{9,10,12,13} The dimeric structure of [(RhClL¹)₂] recalls the chloride-bridged dimeric structure containing two trigonal-bipyramidal rhodium centres suggested for [Rh₂Cl₂{PhP(CH₂CH₂CH=CH₂)₂}]₂.^{17,18} However, the structural assignment

for the latter was made on the basis of NMR evidence and it was concluded that the two bridging chlorine atoms and the phosphorus atom occupied equatorial sites, whilst the two alkenes were mutually *trans* in the axial sites. The equally possible configuration with equatorial alkenes and axial phosphorus and chlorine atoms did not appear to have been considered. The present crystallographic study of the very similar $[(\text{RhClL}^1)_2]$ shows clearly that equatorial alkenes are favoured.

The rhodium–alkene centroid distances (average 2.045 Å) are slightly shorter than those in the cyclic trimer¹² (2.062 Å). The C=C bond lengths (1.40 Å) are also slightly shorter, a reflection again, possibly, of the weaker metal–alkene interaction for silyl alkenes compared to their carbon analogues. The rhodium–chlorine bond lengths in $[(\text{RhClL}^1)_2]$ differ markedly, reflecting their axial [2.392(1) Å] and equatorial [2.588(1) Å] locations. The axial bond length is similar to that observed in the cyclic trimer (2.30 Å, also axial).

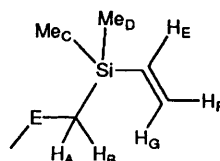
NMR Studies.—Variable-temperature ¹H NMR data for the complexes are reported in Table 6; ¹³C and ²⁹Si NMR data are in Table 7. Energy barrier (ΔG^\ddagger) values are in Table 8. The platinum complexes will be discussed first, followed by the rhodium complexes.

Platinum complexes. For the platinum complexes in the solid state, it is reasonable to assume that each has a structure similar to $[\text{PtL}_2\text{L}^1]$, determined crystallographically. In solution, however, the NMR spectra of the platinum complexes indicate equivalent alkenyl chains at room temperature, an observation inconsistent with the solid-state structure in which the alkenyl chains are in different environments. At low temperature

(−110 °C), though the ¹H spectra are consistent, indicating the presence of two distinguishable alkene moieties: one co-ordinated (¹H resonances at δ 4.0 and 4.6) and one unco-ordinated (resonances at δ 5.6 and 5.8). The spectral changes on raising the temperature are similar to those observed for $[\text{PtX}_2\{\text{S}(\text{CH}_2\text{CH}_2\text{CH}=\text{CH}_2)_2\}]^{10,13}$ and consistent with the exchange of the two alkene moieties, whereby the ligand, rotating about the metal–chalcogen axis, chelates *via* each alkene, consecutively, at the same site. This process has been fully investigated and documented for similar complexes in our earlier papers.^{10,13} Considering the energy barrier to the process of alkene exchange in the complexes $[\text{PtX}_2\text{L}^1]$ and $[\text{PtX}_2\text{L}^2]$, $\Delta G_{\text{Tc}}^\ddagger$ for the process increases in the order $\text{I} < \text{Br} < \text{Cl}$ and $\text{S} < \text{Se}$. The first of these trends is consistent with that established in the study of the dibutenyl chalcogenoether complexes¹⁰ and reflects the greater *trans* effect of the heavier halogen atoms. The second trend, however, is reversed compared with the earlier work, the reason for which is as yet unclear. A comparison between the data for the vinylsilane complexes and the dibutenyl complexes investigated earlier is discussed below.

At still higher temperatures (> 273 K), spectral collapse is again observed for the thioether platinum complexes. The SCH_2 protons, prochiral¹⁹ by virtue of being attached to a chiral chalcogen atom and characterised by two sets of doublets (for $[\text{PtBr}_2\text{L}^1]$: δ 1.94 and 2.34, coupling constant 13.9 Hz) both coupled to platinum [$^3J(^1\text{H}-^{195}\text{Pt})$ 54.3 and 13.6 Hz, respectively] at moderate (fast alkene exchange) temperatures (273 K), give rise to a single broad signal at the coalescence temperature, which sharpens on further warming. This is due to the exchange of the diastereomeric prochiral methylene proton

Table 6 Proton NMR data



$\text{L}^1 \text{ E} = \text{S}$
 $\text{L}^2 \text{ E} = \text{Se}$

(i) ¹H NMR data for alkenyl chain protons in ligands and complexes^a

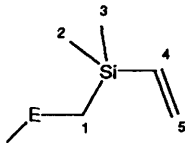
Sample	A	B	C	D	E	F	G
L^1	1.89	1.89	0.16	0.16	6.18	5.98	5.74
L^2	1.82	1.82	0.17	0.17	6.17	5.98	5.73
$[\text{PtCl}_2\text{L}^1]$	2.25	2.30	0.37	0.37	5.28	5.48	5.08
$[\text{PtBr}_2\text{L}^1]$	1.95	2.33	0.37	0.37	5.37	5.58	5.10
$[\text{PtI}_2\text{L}^1]^b$	2.10	2.10	0.36	0.36	5.49	5.70	5.17
$[\text{PtCl}_2\text{L}^2]$	1.96	2.15	0.35	0.39	5.29	5.44	5.00
$[\text{PtBr}_2\text{L}^2]$	1.92	2.19	0.35	0.39	5.40	5.54	5.03
$[\text{PtI}_2\text{L}^2]$	1.84	2.26	0.33	0.37	5.51	5.67	5.11
$[(\text{RhClL}^1)_2]^c$	1.60	1.92	0.18	0.43	4.04	4.39	3.88
$[(\text{RhClL}^2)_2]$	1.81	1.81	0.32	0.39	4.97	5.41	5.41
$[\text{RhCl}(\text{PPh}_3)\text{L}^1]$	1.06	1.33	0.00	0.39	3.63	3.63	3.63

(ii) ¹H NMR data for alkenyl protons at low temperatures^d

Sample	Co-ordinated			Unco-ordinated		
	E	F	G	E	F	G
$[\text{PtCl}_2\text{L}^1]$	4.6	4.0	4.0	5.8	5.6	5.6
$[\text{PtBr}_2\text{L}^1]$	4.8	4.3	4.3	5.9	5.7	5.7
$[\text{PtCl}_2\text{L}^2]$	4.7	4.2	4.2	6.0	5.7	5.7
$[\text{PtBr}_2\text{L}^2]$	4.8	4.4	4.2	6.0	5.7	5.7
$[\text{PtI}_2\text{L}^2]$	5.1	4.6	4.3	6.0	5.7	5.7

^a Recorded at 303 K in CDCl_3 , unless stated otherwise; shifts (δ) relative to SiMe_4 in ppm. ^b At 313 K: coalescence of sulfur inversion process.

^c Alkene assignment uncertain. ^d Recorded at ca. 170 K in CD_2Cl_2 ; for $[\text{PtI}_2\text{L}^1]$, signals are too broad to assign (still exchanging).

Table 7 Carbon-13 and ²⁹Si NMR data *


L¹ E = S
L² E = Se

Sample	¹³ C					²⁹ Si
	1	2	3	4	5	
L ¹	22.74	-3.43	-3.43	137.81	132.38	-7.35
L ²	11.35	-3.02	-3.02	138.07	132.33	-6.67
[PtCl ₂ L ¹]	24.89	-3.17	-2.69	110.26	106.78	1.96
[PtBr ₂ L ¹]	24.66	-3.10	-3.20	110.50	106.60	
[PtI ₂ L ¹]	24.64	-3.34	-2.97	111.10	106.20	
[PtCl ₂ L ²]	17.15	-2.50	-2.32	110	105	
[PtBr ₂ L ²]	17.71	-2.80	-2.46	109.68	105.23	
[(RhCIL ¹) ₂]	32.88	0.03	0.10	59.60	60.94	
[RhCIL ¹ (PPh ₃)]	29.02	0.44	0.44	59.69	63.00	

* Spectra recorded at 303 K in CDCl₃ with shifts (δ) in ppm relative to SiMe₄.

Table 8 Coalescence and energy barrier data from variable-temperature ¹H NMR studies

Complex	Sulfur inversion		Alkene exchange	
	<i>T</i> _c /K	Δ <i>G</i> _{<i>T</i>_c} /kJ mol ⁻¹	<i>T</i> _c /K	Δ <i>G</i> _{<i>T</i>_c} /kJ mol ⁻¹
[PtCl ₂ L ¹]	328	67.29	183	33.8
[PtBr ₂ L ¹]	328	65.96	178	33.0
[PtI ₂ L ¹]	313	61.8	<i>a</i>	<i>a</i>
[PtCl ₂ L ²]	<i>b</i>	<i>b</i>	219	41
[PtBr ₂ L ²]	<i>b</i>	<i>b</i>	210	39
[PtI ₂ L ²]	<i>b</i>	<i>b</i>	193	36

^a Not static at lowest available temperature. ^b Selenium not inverting on NMR time-scale.

environments resulting from pyramidal atomic inversion of the co-ordinated sulfur atom. This process was also observed for the alkenyl thioether complexes previously studied and the phenomenon was first recorded in the mid 1960s.^{20,21} The barrier energies to inversion in the complexes [PtX₂L²] containing the selenoether ligand were too high for analysis by conventional one-dimensional variable-temperature ¹H NMR spectroscopy. For the complexes [PtX₂L¹], where X = Cl or Br, the energies were found to be approximately 10 kJ mol⁻¹ lower than those of their dibutenyl counterparts previously studied.¹⁰ This is comparable with the reduction in alkene exchange barrier energies for the vinylsilane complexes and is likely to be directly linked to this since rapid alkene exchange is considered to facilitate the chalcogen inversion process.¹⁰ The same halogen dependency for the energy barriers, I < Br < Cl, is observed, as for the previously investigated complexes.¹⁰

Comparison between vinylsilane- and butenyl-metal bonding. The infrared spectra of the platinum complexes of the ligands show two absorptions (1594 and 1482 cm⁻¹ for [PtBr₂L¹]) characteristic⁴ of unco-ordinated and co-ordinated vinylsilanes, respectively and corroborate the low-temperature NMR and X-ray evidence for the bidentate nature of the chelate. It is generally accepted²² that the reduction in infrared wavenumber for an alkene upon co-ordination to a metal, Δ*ν*, may be taken as an indication of the strength of the metal-alkene bond. Thus, the greater the Δ*ν*, the stronger the metal-alkene bond. In a previous study of chelating vinylsilanes and their carbon analogues⁴ it was noted that Δ*ν* was smaller for the vinylsilanes than for their carbon counterparts, suggesting that the vinyl-

silane was co-ordinated less strongly to the metal. However, the ¹H NMR chemical shift data for the co-ordinated alkene protons were interpreted as indicating a more significant metal-to-alkene π back-bond in the silyl case. The apparently contradictory infrared and NMR data were rationalised by considering that the σ alkene-to-metal donation was appreciably reduced for the vinylsilane. This was consistent with the proposal that, in vinylsilanes, overlap of silicon d orbitals with the alkene C=C π* orbital provides a more favourable orbital for metal-to-alkene back-bonding^{4,23,24} and also with the fact that the larger silicon atom should render the metallacycle more strained.

In the present work, Δ*ν* for the vinylsilane complexes is typically of the order of 90 cm⁻¹, whereas for the unsubstituted butenyl chain complexes, Δ*ν* is approximately 140 cm⁻¹. The infrared data are thus in accord with the previously discussed investigations.⁴ The work described here, however, allows a more direct comparison of the metal-alkene bond strengths, arising from the quantitative analysis of the fluxional process of alkene exchange (discussed above). It should be noted that a completely rigorous comparison is not strictly possible, since the vinylsilane ligand contains a quaternary silicon atom, whereas the equivalent atom in the butenyl chain¹⁰ is a secondary carbon atom. Nevertheless, it is suggested that the trends discernible in Table 8 are sufficiently unambiguous to render a comparison worthwhile. The energy barrier to alkene exchange, Δ*G*[‡], for the silyl-substituted complexes is about 12 kJ mol⁻¹ less than that for the carbon-containing species,¹⁰ consistent with a more weakly bound alkene in the former complexes. This corroborates the evidence of McCrindle *et al.*⁴ for a weaker metal-alkene interaction for vinylsilane-metal complexes than for their carbon analogues, and is consistent with the conclusion drawn from the X-ray data, above.

Rhodium complexes. The room-temperature ¹H and ¹³C NMR spectra of [(RhCIL¹)₂] are consistent with its crystal structure in that there is only one environment for each hydrogen and carbon nucleus. However, as the temperature is reduced below about 270 K, the ¹H NMR spectra undergo considerable change, particularly in the SiMe₂ region, until at 203 K the strong signals at room temperature are split into about six small signals and two strong signals. This is consistent with the occurrence at room temperature of a fluxional process, which is arrested at low temperature. However, the infrared spectrum shows only one absorption (1474 cm⁻¹) characteristic

of a co-ordinated alkene and no absorption due to unco-ordinated alkene. The fluxional process is therefore different to that occurring in the platinum complexes and whilst it is possible that both alkene functions are co-ordinated at all temperatures in a structure as that determined by X-ray crystallography and that the fluxionality arises from twisting or partial ring reversal in the chelate rings, an alternative explanation could be that in solution, despite the absence of an unco-ordinated alkene, some dissociation and re-coordination of the alkene moieties in a different orientation occurs, thus giving rise to different SiMe environments. At low temperature the fluxional process is arrested giving rise to four chemically distinct geometries, one of which is overwhelmingly favoured and presumably is that observed in the solid-state crystal-structure analysis. The reactions of this compound with other ligands such as phosphines and arsines and the concomitant effects upon structure and fluxionality are under investigation. A preliminary reaction of the thioether dimer with two equivalents of triphenylphosphine at -20°C resulted in the isolation of a yellow crystalline product for which IR, NMR and analytical data are given.

Experimental

General.—Reactions were performed using standard Schlenk techniques under nitrogen (although the platinum products are not noticeably air- or moisture-sensitive) and solvents were dried and distilled under nitrogen before use.

The di(silaalkenyl) thioether ligand, L^1 , was prepared from (chloromethyl)dimethyl(vinyl)silane and sodium sulfide in a two-phase liquid system using tributyl(hexadecyl)phosphonium bromide²⁵ as a phase-transfer catalyst and purified by column chromatography (silica), eluting with hexane.

The di(silaalkenyl) selenoether ligand, L^2 , was prepared by the reaction of sodium selenide (generated *in situ*) with (chloromethyl)dimethyl(vinyl)silane. To a stirred solution of sodium hydroxide (2.553 g, 63.84 mmol) in water (20 cm³) at 50°C was added Rongalite [$\text{Na}(\text{O}_2\text{SCH}_2\text{OH})$] (3.279 g, 21.28 mmol) and selenium powder (0.901 g, 11.42 mmol). After stirring for 1 h (chloromethyl)dimethyl(vinyl)silane (3.075 g, 22.83 mmol) was added dropwise and the mixture was heated under reflux (100°C) for 6 h. After diethyl ether extraction of the cool mixture, drying over magnesium sulfate and purification by column chromatography (silica; eluted using hexane) the ligand L^2 was obtained as a very pale yellow malodorous liquid (2.625 g, 83%).

Preparations of the complexes are exemplified by those of $[\text{PtCl}_2\text{L}^1]$ and $[(\text{RhClL}^2)_2]$.

Preparation of cis-Dichloro(3,3,7,7-tetramethyl-5-thia-3,7-silanon-1,8-diene)platinum(II), $[\text{PtCl}_2\text{L}^1]$.—To a stirring solution of potassium tetrachloroplatinate(II) (1.00 g, 2.41 mmol) in water (10 cm³) and ethanol (3 cm³) was added 1 equivalent of L^1 (0.556 g, 2.41 mmol) in ethanol (2 cm³). The initially clear, red solution turned cloudy pink and was left to stir overnight. After washing the resulting pale yellow precipitate with water, ethanol and diethyl ether and drying *in vacuo*, the product was obtained as a powder in high yield (1.150 g, 96%). The product may be recrystallised from a concentrated dichloromethane solution, or a dichloromethane–hexane two-layer liquid system at -25°C .

The bromo- and iodo-derivatives were prepared by metathesis of the chloro-derivative in warm acetone solution using the appropriate lithium halide.

Preparation of Di- μ -chlorobis[(3,3,7,7-tetramethyl-5-selena-3,7-disilanon-1,8-diene)rhodium(I)], $[(\text{RhClL}^2)_2]$.—To a cold (-80°C) stirred suspension of $[(\text{Rh}(\text{CH}_2=\text{CH}_2)_2\text{Cl})_2]$ (prepared according to ref. 26) (0.300 g, 0.771 mmol) in dichloromethane (40 cm³) were added dropwise 2 equivalents of L^2 (0.428 g, 1.543 mmol) in dichloromethane (2 cm³). The mixture

was stirred and allowed to warm slowly to room temperature overnight. The solvent was removed under reduced pressure from the resulting orange solution and the solid brown material washed with hexane and dried to obtain the crude product. The complex was recrystallised from a dichloromethane–hexane two-layer liquid system.

NMR Studies.— ^1H , ^{13}C and ^{29}Si NMR experiments were performed on a Bruker AM250 spectrometer operating at 250.13, 62.896 and 49.690 MHz, respectively. Low-temperature spectra (-120 to $+30^\circ\text{C}$) were recorded in CD_2Cl_2 . For temperatures up to $+60^\circ\text{C}$, CDCl_3 was employed.

Crystal Structure Determinations of $[\text{PtI}_2\text{L}^1]$ and $[(\text{RhClL}^1)_2]$.—Crystals suitable for X-ray diffraction were grown from dichloromethane–hexane two-layer liquid systems. The crystal data, details of intensity measurements and structure refinement are summarised in Table 9.

All crystallographic measurements were made at 293 K using a Delft Instrument FAST TV area detector diffractometer positioned at the window of a rotating anode generator using Mo-K α radiation ($\lambda = 0.71069 \text{ \AA}$) by following previously described procedures.²⁷ The structures were solved by Patterson methods (SHELX-S)²⁸ and refined by full-matrix least-squares (SHELXL-93)²⁹ using all unique F_o^2 data {excluding two and five 'bad' reflections for $[\text{PtI}_2\text{L}^1]$ and $[(\text{RhClL}^1)_2]$, respectively} corrected for Lorentz and polarisation factors and absorption effects (DIFABS).³⁰ In both cases, the non-hydrogen atoms were refined anisotropically and the hydrogen atoms were included in idealised positions with the U_{iso} parameters tied to the U_{eq} parameters of the parent carbons.

Additional material available from the Cambridge Crystallographic Data Centre comprises H-atom coordinates, thermal parameters and remaining bond lengths and angles.

Table 9 Crystal data and details of data collection and refinement for $[\text{PtI}_2\text{L}^1]$ and $[(\text{RhClL}^1)_2]$

	$[\text{PtI}_2\text{L}^1]$	$[(\text{RhClL}^1)_2]$
Empirical formula	$\text{C}_{10}\text{H}_{22}\text{I}_2\text{PtSi}_2$	$\text{C}_{20}\text{H}_{44}\text{Cl}_2\text{Rh}_2\text{S}_2\text{Si}_4$
M	679.41	737.75
Crystal system	Monoclinic	Triclinic
$a/\text{\AA}$	12.279(5)	7.7178(12)
$b/\text{\AA}$	8.961(3)	10.289(4)
$c/\text{\AA}$	18.575(3)	10.5932(14)
$\alpha/^\circ$	90	92.56(2)
$\beta/^\circ$	108.49(2)	99.544(14)
$\gamma/^\circ$	90	105.26(2)
$U/\text{\AA}^3$	1938.3(10)	769.9(3)
Space group	$P2_1/a$ (no. 14)	$P\bar{1}$
Z	4	1
$D_c/\text{g cm}^{-3}$	2.328	1.537
$F(000)$	1240	376
μ/cm^{-1}	106.4	14.13
Crystal size/mm	$0.35 \times 0.28 \times 0.16$	$0.29 \times 0.25 \times 0.18$
θ range for data/ $^\circ$	2.31–30.03	2.97–30.23
$h_{\text{min}}, h_{\text{max}}$	–12, 17	–7, 10
$k_{\text{min}}, k_{\text{max}}$	–10, 12	–14, 10
$l_{\text{min}}, l_{\text{max}}$	–24, 20	–14, 10
Total data measured	9638	4027
Total unique (R_{int})	4849 (0.0645)	3633 (0.0392)
No. of parameters/data	149/4849	140/3628
Absorption correction	0.760/1.144	0.968/1.060
factors, min./max.		
Goodness-of-fit on F_o^2	0.458	0.349
$\rho_{\text{min}}, \rho_{\text{max}}/\text{e \AA}^{-3}$	–0.871, 1.122	–0.466, 0.509
R_1^*	0.100 (0.039)	0.045 (0.030)
wR_2^*	0.169 (0.092)	0.106 (0.075)

* $R_1 = \Sigma(F_o - F_c)/\Sigma(F_o)$; $wR_2 = \{\Sigma[w(F_o^2 - F_c^2)^2]/\Sigma[w(F_o^2)^2]\}^{1/2}$; $w = 1/[\sigma^2(F_o^2)]$; R_1 and wR_2 values for data with $I > 2\sigma(I)$ (1676 for the Pt and 2223 for the Rh complex) are given in parentheses.

Acknowledgements

We thank the Royal Society for the award of a Return Fellowship (Japan) to J. R. K. and the SERC for support of the Crystallography Service at the University of Wales College of Cardiff.

References

- 1 D. C. Goodall, *J. Chem. Soc. A*, 1966, 1562.
- 2 D. C. Goodall, *J. Chem. Soc. A*, 1968, 887.
- 3 D. C. Goodall, *J. Chem. Soc. A*, 1969, 890.
- 4 R. McCrindle, E. A. Alyea, S. A. Dias and A. J. McAlees, *J. Chem. Soc., Dalton Trans.*, 1979, 640.
- 5 R. McCrindle, E. C. Alyea, G. Ferguson, S. A. Dias, A. J. McAlees and M. Parvez, *J. Chem. Soc., Dalton Trans.*, 1980, 137.
- 6 E. C. Alyea, G. Ferguson, A. J. McAlees, R. McCrindle, R. Myers, P. Y. Siew and S. A. Dias, *J. Chem. Soc., Dalton Trans.*, 1981, 481.
- 7 D. T. Clark, K. B. Dillon, H. R. Thomas and T. C. Waddington, *J. Chem. Soc., Dalton Trans.*, 1979, 250.
- 8 N. L. Allinger and V. Zalkow, *J. Org. Chem.*, 1960, 25, 701.
- 9 E. W. Abel, D. G. Evans, J. R. Koe, V. Sik, P. A. Bates and M. B. Hursthouse, *J. Chem. Soc., Dalton Trans.*, 1989, 985.
- 10 E. W. Abel, D. G. Evans, J. R. Koe, V. Sik, P. A. Bates and M. B. Hursthouse, *J. Chem. Soc., Dalton Trans.*, 1989, 2315.
- 11 E. W. Abel, D. G. Evans, J. R. Koe, M. B. Hursthouse, M. Mazid, M. F. Mahon and K. C. Molloy, *J. Chem. Soc., Dalton Trans.*, 1990, 1697.
- 12 E. W. Abel, D. G. Evans, J. R. Koe, V. Sik, M. B. Hursthouse and M. Mazid, *Polyhedron*, 1992, 11, 401.
- 13 E. W. Abel, D. G. Evans, J. R. Koe, M. B. Hursthouse and M. Mazid, *J. Chem. Soc., Dalton Trans.*, 1992, 663.
- 14 R. R. Ryan, R. Schaeffer, P. W. Clark and G. E. Hartwell, *Inorg. Chem.*, 1975, 14, 3039.
- 15 M. O. Visscher, J. C. Huffmann and W. E. Streit, *Inorg. Chem.*, 1974, 13, 792.
- 16 T. A. Albright, R. Hoffmann, J. C. Thibeault and D. L. Thorn, *J. Am. Chem. Soc.*, 1979, 101, 3801.
- 17 P. W. Clark and G. E. Hartwell, *J. Organomet. Chem.*, 1975, 96, 451.
- 18 P. W. Clark, P. Hanisch and A. J. Jones, *Inorg. Chem.*, 1979, 18, 2067.
- 19 W. B. Jennings, *Chem. Rev.*, 1975, 75, 307.
- 20 E. W. Abel, R. P. Bush, F. J. Hopton and C. R. Jenkins, *Chem. Commun.*, 1966, 58.
- 21 P. Haake and P. C. Turley, *J. Am. Chem. Soc.*, 1967, 89, 4611.
- 22 R. S. Nyholm, *Rev. Pure Appl. Chem.*, 1971, 27, 127.
- 23 I. Haiduc and V. Popa, *Adv. Organomet. Chem.*, 1977, 15, 115.
- 24 J. W. Fitch, D. P. Flores and J. E. George, *J. Organomet. Chem.*, 1971, 29, 263.
- 25 D. Landini and F. Rolla, *Synthesis*, 1974, 565.
- 26 R. Cramer, *Inorg. Synth.*, 1974, 15, 14.
- 27 J. A. Darr, S. R. Drake, M. B. Hursthouse and K. M. A. Malik, *Inorg. Chem.*, 1993, 32, 5704.
- 28 G. M. Sheldrick, *Acta Crystallogr., Sect. A*, 1990, 46, 467.
- 29 G. M. Sheldrick, *J. Appl. Crystallogr.*, in the press.
- 30 N. Walker and D. Stuart, *Acta Crystallogr., Sect. A*, 1983, 39, 158, adapted for FAST Geometry by A. Karaulov, University of Wales, Cardiff, 1991.

Received 15th March 1994; Paper 4/01562B